Experimental and numerical study of MILD combustion in a lab-scale furnace

Huang, Xu; Tummers, M. J.; Roekaerts, D. J.E.M.

DOI
10.1016/j.egypro.2017.07.231

Publication date
2017

Document Version
Final published version

Published in
Proceedings of the 11th European Conference on Industrial Furnaces and Boilers (INFUB-11)

Available online at www.sciencedirect.com

ScienceDirect

Energy Procedia 120 (2017) 395–402

Energy Procedia

www.elsevier.com/locate/procedia

INFUB - 11th European Conference on Industrial Furnaces and Boilers, INFUB-11

Experimental and numerical study of MILD combustion in a lab-scale furnace

X. Huang[a]*, M.J. Tummers[a], and D.J.E.M. Roekaerts[a]

[a]*Fluid Mechanics Section, Department of Process and Energy, Delft University of Technology, Leeghwaterstraat 39, Delft, 2628CB, The Netherlands*

Abstract

Mild combustion in a lab-scale furnace has been experimentally and numerically studied. The furnace was operated with Dutch natural gas (DNG) at 10 kW and at an equivalence ratio of 0.8. OH* chemiluminescence images were taken to characterize the reaction zone. The chemiluminescence intensity is relatively low compared to conventional flames and relatively uniformly distributed in the reaction zone due to the dilution effects of recirculated burnt gases. Visible flames were not observed. To characterize the dilution effects of burnt gases on reactions, flamelets generated with diluted fuel and diluted air, instead of flamelets based on pure fuel and air, were applied in an extended Flamelet Generated Manifold (FGM) approach. Burnt gases at stoichiometric mixture fraction rather than those at global equivalence ratio were considered as diluent, which is more appropriate for furnaces operating at lean condition. The numerical simulations were performed using the open source CFD package -- OpenFOAM.

Peer-review under responsibility of the organizing committee of INFUB-11

Keywords: MILD; flameless; turbulent combustion; furnace; NOx; OpenFOAM

1. Introduction

Recycling the waste heat of flue gas is a way to improve the thermal efficiency of combustion systems, but unfortunately, it leads to higher temperature which has an adverse effect on nitrogen oxides (NOx) formation.

* Corresponding author
E-mail address: x.huang-2@tudelft.nl

1876-6102
Peer-review under responsibility of the organizing committee of INFUB-11
10.1016/j.egypro.2017.07.231

Maintaining low reaction temperature is an effective way to reduce NO_x formation. Moderate or Intense Low-oxygen Dilution (MILD) combustion, also named flameless combustion or high-temperature air combustion (HiTAC), works on the principle of diluting reactants with recirculated combustion products slowing down the reactions. Reaction intensity is low and heat release is distributed over a large space which results in reduced peak flame temperature and less NO_x formation.

MILD combustion can occur when fresh air (and/or fuel) streams are sufficiently diluted by entrained combustion products before reactions take place, as shown in the regime diagram proposed in ref.[1]. MILD combustion has recently been experimentally studied on laboratory-scale setups because of scientific challenges, environmental concerns and its potential industrial applications. Three levels of experimental setup are used to study MILD combustion. Those are jet-in-hot-coflow burners[2,3], lab-scale furnaces[4-7] and semi-industrial furnaces[8,9]. Compared to the jet-in-hot-coflow burner, in a lab-scale furnace the internal recirculation patterns are represented more faithfully but the configuration is still simple enough to make detailed laser diagnostic measurements, in contrast with the more complex (semi-)industrial furnaces. Here we report on first results in a new lab-scale furnace. To obtain detailed measurements to reveal the nature of the combustion process, the lab-scale furnace presented in this study is designed to provide full optical access to perform OH* chemiluminescence, Laser Doppler Anemometry (LDA), Particle Velocity Velocimetry (PIV), Planar Laser-Induced Fluorescence (PLIF) and Coherent Anti-Stokes Raman Spectroscopy (CARS) measurements.

MILD regime is often claimed to occur at Damköhler number (Da) of an order of unity where flamelet concept is not valid and the Eddy Dissipation Concept (EDC) model is often applied to MILD combustion modeling in furnaces[10,11]. Nevertheless, experimental results especially PLIF images[4,12,13] have shown the presence of thin reaction zones or flamelets in MILD combustion. Recent DNS (Direct Numerical Simulation) results also have shown that typical flamelet-like thin reaction zones do exist in MILD combustion[14,15]. Flamelet based models such as Flamelet Generated Manifolds (FGM) approach therefore could still be attractive for MILD combustion also because these are requiring less computational resources while incorporating detailed chemistry[16,17]. The challenge of modelling MILD combustion in furnaces with the FGM approach is to include in a proper way the dilution effects by recirculated burnt gases. Dilution effects were taken into account by using diluted flamelets [18-20], but differently from those works here the diluent is not considered as the burnt gases at global equivalence ratio but as the burnt gases at stoichiometric conditions, which is more appropriate in the tabulation of possible states in the furnace.

The aim of this work is to obtain more insights on MILD combustion and extend the range of operational conditions in MILD regime based on experiments and numerical modeling. This paper reports reaction characteristics in the current furnace indicated by the OH* chemiluminescence images. In numerical modeling, an extended FGM approach including dilution effects of burnt gases was implemented in the open source CFD package OpenFOAM. In order to tabulate more possible states in furnace, dilution effects were taken into account by burnt gases at stoichiometric mixture fraction. Radiation model was also implemented with the extended FGM approach.

2. Experimental setup

The lab-scale furnace built in Delft University of Technology has a 320 mm × 320 mm square cross section and a height of 630 mm, as shown in Fig. 1. The combustion chamber is made of ceramically bonded vermiculite plates, which are 50 mm thick for the sides and bottom, 25 mm for the top. A commercial REKUMAT 150 recuperative Flame-FLOX burner is placed at the bottom of the combustion chamber. The burner nozzles are protruding 30 mm into the chamber, and the distance from nozzle tip to furnace top is 600 mm. The injectors consist of one central fuel nozzle with a diameter of 4.5 mm and 4 air nozzles with a diameter of 8.6 mm symmetrically located around the fuel nozzle. Dutch natural gas (DNG, typical composition in volume fraction being 0.813 CH_4, 0.037 C_2H_6, 0.144 N_2, 0.006 rest) is used as fuel. Flow rates are controlled by mass flow controllers. The heat extraction can be controlled by blowing cooling air on the top plate. This cooling method is chosen because it causes less flow complexity than internal cooling tubes. The furnace is designed to work in both premixed flame mode and MILD mode. Flame mode is used to heat up the furnace to 1123 K. In flame mode, fuel and air are premixed and injected into the furnace through the four air nozzles. Premixed flames stabilize on the four air nozzles. Once the temperature inside the furnace is above 1123 K, the furnace switches to MILD mode where the fuel is injected through the central fuel

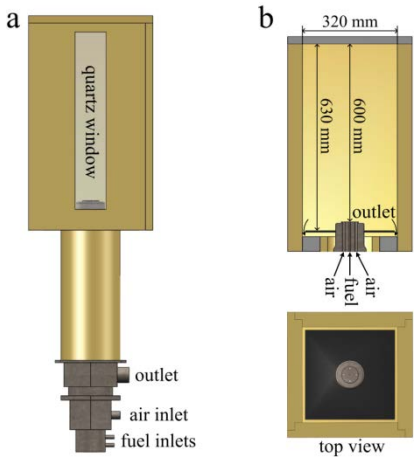

Fig. 1. Schematic of the lab-scale MILD furnace, a: complete furnace; b: cross sections of combustion chamber: vertical mid-plane (top) and horizontal plane at injector level (bottom).

nozzle and only air via the air nozzles. Due to the discrete injection of fuel and air, sufficient burnt gases are entrained into fuel and air jets. Fuel and air are diluted and preheated before reactions take place. MILD regime is established in this way. Flue gases leave the chamber through a slit between the side walls and the bottom plate as shown in Fig. 1b(bottom). The flue gases are then introduced into the recuperator of the burner to preheat air. The recuperator is able to preheat air up to 973 K. One vertical wall is equipped with a quartz window of size 105 mm × 600 mm to provide optical access for OH* chemiluminescence.

The furnace was operating at 10 kW and at different equivalence ratios. The OH* chemiluminescence images were collected with an intensified high-speed camera at 3 different heights (from 290 mm to 560 mm above the nozzle) and then the whole measured region was reconstructed. In order to obtain longer averaging time, 3000 frames were taken at 50 fps at each height.

3. Modeling approach

3.1. Model details

The combustion in furnace can be described as a three-stream problem, with flammable mixtures created from fuel, air and recirculated flue gas. Flamelets with only fuel and air as inflow do not take into account the dilution effects by burnt gases on the flame structure. Fig. 2 shows an example of the dilution effects on reactions. It shows the mass fraction curves of methane and carbon dioxide in the tabulated flamelet table generated by laminar counterflow flame at different dilution conditions. It can be seen that although reactants and products converge to the final near equilibrium state, reactions follow different paths. This means flame structures are different at different dilution conditions. To handle this, new chemistry tabulation methods including dilution effects in flamelets have been proposed [18,19]. The fuel and oxidizer at the laminar counterflow flame boundaries are replaced by fuel and oxidizer diluted by burnt gases at global equivalence ratio of the furnace operation. A dilution level is used to describe the mass fraction of diluent in the local instantaneous gas mixture. Diluted fuel and diluted oxidizer are considered to have the same mass fraction of diluent. In this way, the mixture fraction Z of local instantaneous gas mixture is written as:

$$Z = (1-\alpha) Z_{\alpha} + \alpha Z_{d} \tag{1}$$

where α is the dilution level denoting the mass fraction of diluent in local instantaneous gas mixture, Z_{α} is mixture fraction of unburnt fuel and air at dilution level α, and Z_d is the mixture fraction of diluent evaluated at global

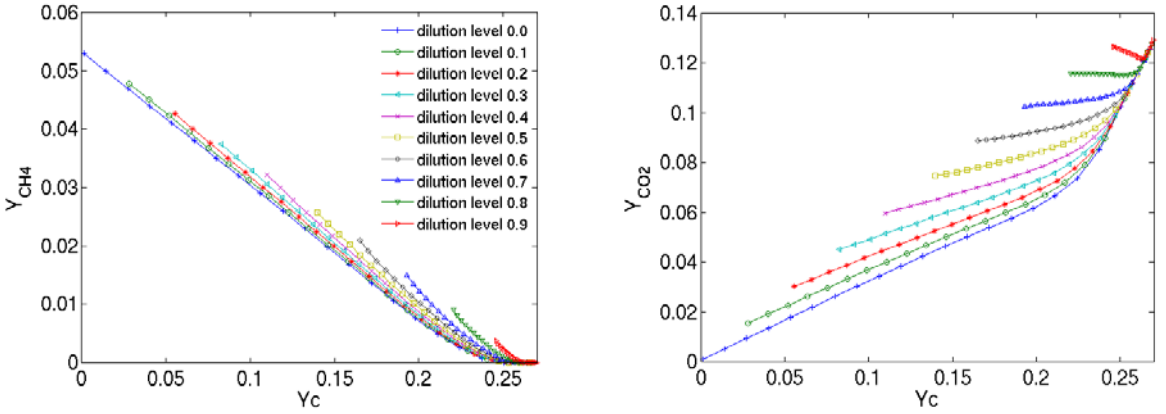

Fig. 2. CH_4 and CO_2 mass fraction as function of reaction progress variable at stoichiometric mixture fraction at different dilution levels.

equivalence ratio.

A dilution variable Y_d is defined as a combination of species mass fraction, i.e. $Y_d=Y_{CO}+Y_{CO2}$. The dilution level α is related to the dilution variable by the following equation:

$$\alpha = \frac{Y_d}{Y_{d,dil}} \tag{2}$$

where $Y_{d,dil}$ denotes the dilution variable in pure diluent.

However, defining the burnt gases at global equivalence ratio as diluent stream is not a good choice for furnaces operating at lean condition. There are two reasons. Firstly, when a fuel jet is entering the furnace, fuel may react with the hot air left in the burnt gases immediately before it mixes with fresh air. With diluent defined as burnt gases at global equivalence ratio, only the mixing state of fuel and diluent is tabulated in the tables. Therefore reactions between fuel and air in diluent are not predicted. Secondly, when unburnt fuel and air locally form a mixture very close to stoichiometric mixture fraction, and then are diluted, the diluent species mass fractions can grow to values corresponding to an unacceptable value $\alpha=Y_d/Y_{d,dil}$ is larger than 1.

To overcome this issue, to define diluent as burnt gases at stoichiometric mixture fraction is proposed in the study. Chemically inert combustion products, i.e. CO_2, H_2O and N_2 are treated as diluent species. Burnt gases at global equivalence ratio then can be considered as consisting of reaction products at stoichiometric condition and excess air. The mixture fraction Z of local instantaneous gas mixture is written as:

$$Z = (1-\alpha) Z_\alpha + \alpha Z_{st} \tag{3}$$

where Z_{st} is the stoichiometric mixture fraction of pure fuel and air, and $\alpha=Y_d/Y_{d,st}$, $Y_{d,st}$ is the dilution variable in burnt gases at Z_{st}.

An enthalpy loss factor η is used to account for enthalpy loss due to the heat transfer to the furnace walls. Maximum enthalpy loss happens at η=1, and no enthalpy loss at η=0. The enthalpy of gas mixture h is the sum of that of diluent and fuel/air mixture. Enthalpy in diluent h_{dil} with enthalpy loss is

$$h_{dil} = h_{dil,\eta=0} + \eta\left(h_{dil,\eta=1} - h_{dil,\eta=0}\right) \tag{4}$$

Enthalpy of fuel/air mixture $h_{f/ox}$ is

$$h_{f/ox} = h_{ox,\alpha=0} + Z_\alpha \left(h_{f,\alpha=0} - h_{ox,\alpha=0}\right) \tag{5}$$

The enthalpy of gas mixture h is then written as:

$$h = (1-\alpha)h_{f/ox} + \alpha h_{dil} \tag{6}$$

By combining equations (4), (5) and (6), enthalpy loss factor η can written as:

$$\eta = \frac{h_{dil} - h_{dil,\eta=0}}{h_{dil,\eta=1} - h_{dil,\eta=0}} = \frac{h - h_{\eta=0}}{\alpha\left(h_{dil,\eta=1} - h_{dil,\eta=0}\right)} \tag{7}$$

For the scaled reaction progress variable c, it should be evaluated at local dilution level α and reaction progress variable Y_c. Therefore, the scaled progress variable is a function of local fuel/air mixture fraction, scaled dilution variable and enthalpy loss factor and is written as:

$$c = \frac{Y_c - Y_{c,u}\left(Z_\alpha, \alpha, \eta\right)}{Y_{c,b}\left(Z_\alpha, \alpha, \eta\right) - Y_{c,u}\left(Z_\alpha, \alpha, \eta\right)} \tag{8}$$

where $Y_{c,b}(Z_\alpha, \alpha, \eta)$ and $Y_{c,u}(Z_\alpha, \alpha, \eta)$ are the progress variable in burnt gases and unburnt gases, respectively.

To this end, all thermochemical quantities are tabulated in terms of mixture fraction, scaled progress variable, dilution level and enthalpy loss factor. Quantities in the lookup tables become four dimensional and are written as:

$$\Phi = \Phi\left(Z_\alpha, c, \alpha, \eta\right) \tag{9}$$

Taking into account turbulence/chemistry interactions by a presumed β-function PDF for mixture fraction Z_α and scaled progress variable c, the thermochemical quantities in RANS simulation are tabulated as:

$$\widetilde{\Phi} = \widetilde{\Phi}\left(\widetilde{Z_\alpha}, \widetilde{Z_\alpha''^2}, \tilde{c}, \widetilde{c''^2}, \alpha, \eta\right) \tag{10}$$

With the solutions of the following Favre-averaged equations, six table control parameters can be evaluated.

$$\frac{\partial \overline{\rho}\widetilde{Z}}{\partial t} + \frac{\partial}{\partial t}\left(\overline{\rho}\widetilde{u_i}\widetilde{Z}\right) = \frac{\partial}{\partial x_i}\left[\left(\overline{\rho}D + \frac{\mu_t}{Sc_t}\right)\frac{\partial \widetilde{Z}}{\partial x_i}\right] \tag{11}$$

$$\frac{\partial \overline{\rho}\widetilde{Y_c}}{\partial t} + \frac{\partial}{\partial t}\left(\overline{\rho}\widetilde{u_i}\widetilde{Y_c}\right) = \frac{\partial}{\partial x_i}\left[\left(\overline{\rho}D + \frac{\mu_t}{Sc_t}\right)\frac{\partial \widetilde{Y_c}}{\partial x_i}\right] + \overline{\dot{\omega}}_{Y_c} \tag{12}$$

$$\frac{\partial \overline{\rho}\tilde{h}}{\partial t} + \frac{\partial}{\partial t}\left(\overline{\rho}\widetilde{u_i}\tilde{h}\right) = \frac{\partial}{\partial x_i}\left[\left(\overline{\rho}D + \frac{\mu_t}{Sc_t}\right)\frac{\partial \tilde{h}}{\partial x_i}\right] + S_h \tag{13}$$

$$\frac{\partial \overline{\rho}\widetilde{Y_d}}{\partial t} + \frac{\partial}{\partial t}\left(\overline{\rho}\widetilde{u_i}\widetilde{Y_d}\right) = \frac{\partial}{\partial x_i}\left[\left(\overline{\rho}D + \frac{\mu_t}{Sc_t}\right)\frac{\partial \widetilde{Y_d}}{\partial x_i}\right] + \overline{\dot{\omega}}_{Y_d} \tag{14}$$

$$\frac{\partial \overline{\rho}\widetilde{Z''^2}}{\partial t} + \frac{\partial}{\partial t}\left(\overline{\rho}\widetilde{u_i}\widetilde{Z''^2}\right) = \frac{\partial}{\partial x_i}\left[\left(\overline{\rho}D + \frac{\mu_t}{Sc_t}\right)\frac{\partial \widetilde{Z''^2}}{\partial x_i}\right] + 2\frac{\mu_t}{Sc_t}\frac{\partial \widetilde{Z}}{\partial x_i}\frac{\partial \widetilde{Z}}{\partial x_i} - C_{dz}\overline{\rho}\frac{\tilde{\varepsilon}}{\tilde{k}}\widetilde{Z''^2} \tag{15}$$

$$\frac{\partial \overline{\rho}\widetilde{Y_c''^2}}{\partial t} + \frac{\partial}{\partial t}\left(\overline{\rho}\widetilde{u_i}\widetilde{Y_c''^2}\right) = \frac{\partial}{\partial x_i}\left[\left(\overline{\rho}D + \frac{\mu_t}{Sc_t}\right)\frac{\partial \widetilde{Y_c''^2}}{\partial x_i}\right] + 2\frac{\mu_t}{Sc_t}\frac{\partial \widetilde{Y_c}}{\partial x_i}\frac{\partial \widetilde{Y_c}}{\partial x_i} - C_{dY_c}\overline{\rho}\frac{\tilde{\varepsilon}}{\tilde{k}}\widetilde{Z''^2} + 2\left(\overline{Y_c\dot{\omega}_{Y_c}} - \widetilde{Y_c}\overline{\dot{\omega}}_{Y_c}\right) \tag{16}$$

In these equations, ρ is the mean density, D is the molecular diffusion coefficient, μ_t is the turbulent viscosity, Sc_t is the turbulent Schmidt number, $\dot{\omega}_{Yc}$ is the chemical source term of the progress variable, $\dot{\omega}_{Yd}$ is the source term of the dilution variable, C_{dz} and C_{dYc} are model constants, k is the turbulent kinetic energy and ε is the turbulent dissipation rate. In the equations given above, the gradient transport assumption[21] coupled with unit Lewis numbers for all variables have been used to model the diffusion terms. The source term $\dot{\omega}_{Yd}$ in dilution variable transport equation (14) is providing the transformation of burnt gases at local mixture fraction into diluent stream when reaction is completed which means scaled reaction progress variable equals to 1. Different forms of this term can be found in Ref. [18, 19].

3.2. Simulation setup

Numerical simulations have been performed for the case when the furnace is operated at 10 kW at global equivalence ratio 0.8, without and with radiation heat transfer (P1 method with constant absorption coefficient). Due to lack of detailed experimental data, inlet temperatures of fuel and air were estimated at 350 K and 673 K based on the mass flow rates and injection velocities. The wall temperature is estimated at 1200 K based on the furnace in ref. [5,6] working at similar conditions. The six dimensional lookup tables were computed with 51×11×51×11×11×3 grid points in the direction of mixture fraction, mixture fraction variance, scaled progress variable, scaled progress variable variance, dilution level and heat loss parameter, respectively. Due to symmetry only half of the furnace is considered as the computational domain. (The fourfold symmetry reduces to a mirror symmetry when the presence of a window at one side only is taken into account.)

4. Results and discussion

Fig. 3 shows the furnace works in flame mode (Fig. 3a), MILD mode (Fig. 3b) and mean OH* chemiluminescence at equivalence ratio 0.8 (Fig. 3c). The NO_x emission measured in flame mode is above 50 ppm, but it was below 1 ppm in MILD mode. For the current furnace configuration, the outlet in the bottom plane and the high momentum air injection are favourable for the generation of reverse flow, which is decisive to achieve MILD combustion. Burnt gases flow back to the inlets and are entrained into the fuel and air jets. Fuel and air streams are diluted and preheated by burnt gases before mixing. Once they are hot enough and well mixed, ignition starts. Due to long mixing process, reactions take place in diluted conditions in a distributed zone as shown in Fig.3c.

Fig. 4 shows the mean OH* chemiluminescence images at different equivalence ratio ϕ. The vertical axis in the image indicates the height above the burner head and the horizontal axis shows the offset from the central line of fuel jet. In the case ϕ=0.7, the reaction zone is between 300~560 mm and the OH* chemiluminescence intensity is the lowest of the three cases. As equivalence ratio increases, the reaction zone shifts downstream, and OH*

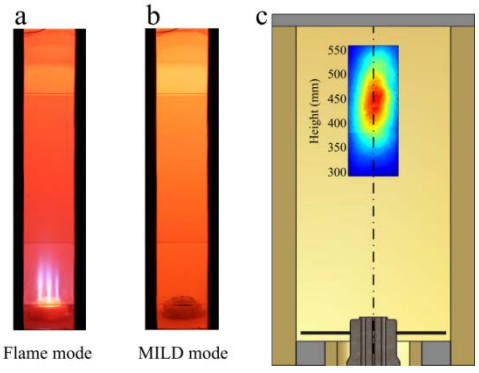

Fig. 3. (a) furnace operating in flame mode; (b) furnace operating in MILD mode; (c) mean OH* chemiluminescence image.

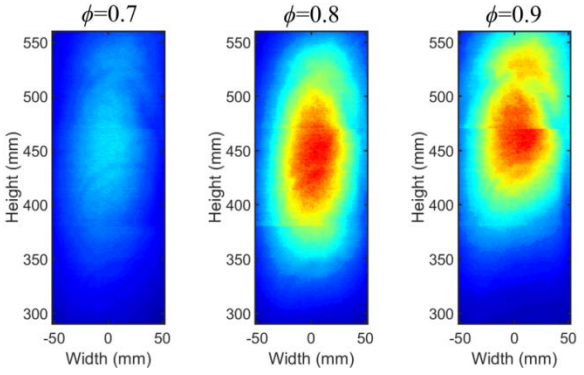

Fig. 4. Mean OH* chemiluminescence at different equivalence ratios.

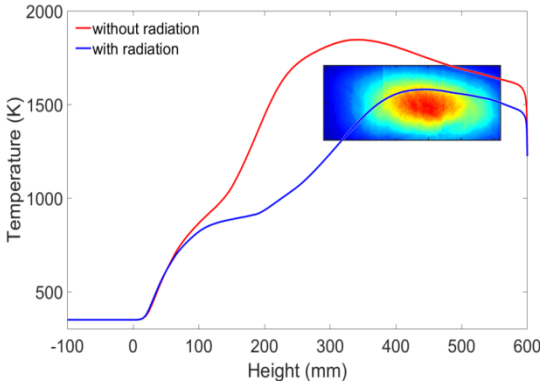

Fig. 5. Temperature profiles along the fuel central line.

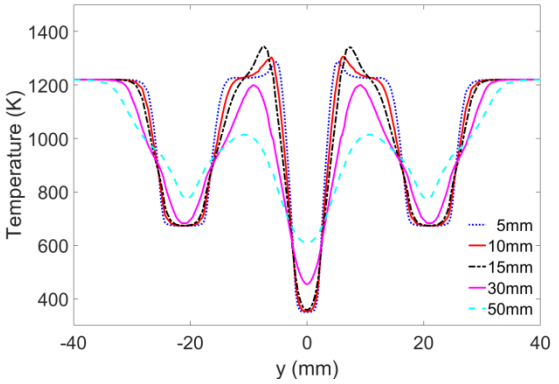

Fig. 6. Mean temperature profiles near nozzle exit.

chemiluminescence intensity becomes higher. This shift of main reaction zone is due to the decrease in air jets momentum when increasing equivalence ratio. Decreasing air jets velocity results in less entrainment of burnt gases. On the one hand, fuel and air need longer preheating time to reach ignition temperature and therefore reactions are delayed. On the other hand, less entrainment of burnt gases means less dilution which leads to higher reaction intensity. When decreasing equivalence ratio, faster entrainment of burnt gases by high momentum air jets reduces preheating time and increases the dilution. The reaction zone shift upstream and reaction intensity decrease. It is concluded that the current laboratory-scale furnace is quite robustly operating in MILD combustion regime.

Fig. 5 shows the predicted temperature profiles along the fuel central line with and without radiation model. When radiation effects are included, the peak temperature decreases by about 265 K, which means radiation significantly influencing the heat transfer inside the furnace and should be taken into account. Due to radiation heat loss at walls, flue gas temperature is lower which lead slower fuel and air preheat and reaction is delayed. Due to the lack of experimental data, only the predicted high temperature zone is compared with OH* chemiluminescence measurements. As shown in Fig. 5, the high temperature zone predicted with consideration of radiation hear transfer is consistent with OH* chemiluminescence measurements (OH* is usually used to indicate reaction zone).

As mentioned previously, the model proposed is capable to capture the reaction between fuel and excess air in recirculated burnt gases. Fig. 6 shows the predicted temperature profiles at 5 mm, 10 mm, 15 mm, 30 mm and 50 mm above the nozzle exit in the mid-plane without radiation model. Two temperature peaks at the fuel jet boundary were observed in each profile. The temperature values at the peaks increase and move outwards as the fuel jet develops. This is due to the reaction between fuel and excess air because of the lean operating condition of the furnace. As getting further away from the nozzle, the reaction between fuel and excess air in the burnt gases is influenced by freshly injected air. The temperature in the region starts decreasing, as shown in the temperature profiles at 15 mm, 30 mm and 50 mm in Fig. 6. Jets temperatures are increasing due to mixing with entrained burnt gases.

5. Conclusions

MILD combustion was successfully achieved in a lab-scale furnace with a recuperative burner with NO_x below 1 ppm. The reaction zone is visualised by OH* chemiluminescence measurements. The reaction intensity in MILD combustion is much lower than that in conventional flames. As equivalence ratio decreases, the air jets velocity increases results in more entrainment of burnt gases, that is better dilution. Reaction zone shifts upstream, and OH* chemiluminescence intensity becomes higher. To define diluent as chemically inert products at stoichiometric mixture fraction to generate diluted flamelets is more appropriate for furnaces working at fuel lean condition. The reactions between fresh fuel and air left in burnt gases are predicted when fuel enters the furnace. The high temperature zone predicted by the model is consistent with the reaction zone indicated by OH* chemiluminescence measurements. Radiation significantly influences the heat transfer inside the furnace therefore be included in the simulation.

Acknowledgements

The authors would like to thank the China Scholarship Council (CSC) for financial support for the first author. The authors acknowledge funding by Technology Foundation STW for the construction of the furnace. This work was sponsored by NWO Physical Sciences for the use of HPC resources.

References

[1] Wunning JA, Wunning JG. Flameless oxidation to reduce thermal no-formation. Progress in Energy and Combustion Science 1997; 23: 81-94.
[2] Oldenhof E, Tummers MJ, van Veen EH, Roekaerts DJEM. Ignition kernel formation and lift-off behaviour of jet-in-hot-coflow flames. Combustion and Flame 2010; 157: 1167-1178.
[3] Dally BB, Karpetis AN, Barlow RS. Structure of turbulent non-premixed jet flames in a diluted hot coflow. Proceedings of the Combustion Institute 2002; 29: 1147-1154.
[4] Plessing T, Peters N, Wunning JG. Laseroptical investigation of highly preheated combustion with strong exhaust gas recirculation. Twenty-Seventh Symposium (International) on Combustion/The Combustion Institute 1998; 3197-3204
[5] Szegö GG, Dally BB, Nathan GJ. Scaling of NOx emissions from a laboratory-scale mild combustion furnace. Combustion and Flame 2008; 154: 281-295.
[6] Veríssimo AS, Rocha AMA, Costa M. Operational, combustion, and emission characteristics of a small-scale combustor. Energy & Fuels 2011; 25: 2469-2480.
[7] Lupant D, Pesenti B, Lybaert P. Influence of probe sampling on reacting species measurement in diluted combustion. Experimental Thermal and Fluid Science 2010; 34: 516-522.
[8] Mancini M, Weber R, Bollettini U. Predicting NOx emissions of a burner operated in flameless oxidation mode. Proceedings of the Combustion Institute 2002; 29: 1155-1163.
[9] Cho ES, Shin D, Lu J, de Jong W, Roekaerts DJEM. Configuration effects of natural gas fired multi-pair regenerative burners in a flameless oxidation furnace on efficiency and emissions. Applied Energy 2013; 107: 25-32.
[10] Li P, Mi J, Dally BB, Craig RA, Wang F. Premixed moderate or intense low-oxygen dilution (MILD) combustion from a single jet burner in a laboratory-scale furnace. Energy & Fuels 2011; 25: 2782-2793.
[11] Graça M, Duarte A, Coelho PJ, Costa M. Numerical simulation of a reversed flow small-scale combustor. Fuel Processing Technology 2013; 107: 126-137.
[12] Dally BB, Riesmeier E, Peters N. Effect of fuel mixture on moderate and intense low oxygen dilution combustion. Combustion and Flame 2004; 137: 418-431.
[13] Ozdemir IB, Peters N. Characteristics of the reaction zone in a combustor operating at mild combustion. Expeiments in Fluids 2001; 30: 683-695.
[14] Minamoto Y, Swaminathan N, Cant RS, Leung T. Reaction zones and their structure in MILD combustion. Combustion Science and Technology 2014; 186: 1075-1096.
[15] Minamoto Y, Swaminathan N. Scalar gradient behaviour in MILD combustion. Combustion and Flame 2014; 161: 1063-1075.
[16] Peters N. Laminar diffusion flamelet models in non-premixed turbulent combustion. Prog. Energy Combust. Sci. 1984; 10.
[17] Oijen JAV, Goey LPHD. Modelling of premixed laminar flames using flamelet-generated manifolds. Combustion Science and Technology 2000; 161: 113-137.
[18] Lamouroux J, Ihme M, Fiorina B, Gicquel O. Tabulated chemistry approach for diluted combustion regimes with internal recirculation and heat losses. Combustion and Flame 2014; 161: 2120-2136.
[19] Colin O, Michel J-B. A two-dimensional tabulated flamelet combustion model for furnace applications. Flow, Turbulence and Combustion 2016.
[20] Locci C, Colin O, Poitou D, Mauss F. A tabulated, flamelet based no model for large eddy simulations of non-premixed turbulent jets with enthalpy loss. Flow, Turbulence and Combustion 2015; 94: 691-729.
[21] Poinsot T, Veynante D, Theoretical and numerical combustion (Third Edition). 2012, Bordeaux, France: Aquaprint.